

Proceedings of the 2nd Winter Workshop S&SRES'96, Polanica Zdrój 1996

ENERGY TRANSFER, FLUORESCENCE AND SCINTILLATION PROCESSES IN CERIUM-DOPED $RE^{3+}AlO_3$ FAST SCINTILLATORS

J.A. MARES AND M. NIKL

Institute of Physics, Czech Academy of Sciences
Cukrovarnicka 10, 16200 Prague 6, Czech Republic

Modern applications of scintillators in medical imaging of human body (Positron Emission Tomography — PET scanning, γ -cameras and other X-ray tomographies) require improved or even quite new scintillators which should be characterized by (i) fast response, (ii) high density and (iii) high light yield. At present time new scintillating crystals are investigated, mainly those having perovskite lattice structure of the formula $RE^{3+}AlO_3:Ce$ where $RE^{3+} = Y^{3+}, Gd^{3+}$ and Lu^{3+} . Here, we will present the newest data with summarising properties of these types of scintillators including the mixed ones. Energy transfer processes between Ce^{3+} main centres and Ce^{3+} multsites are discussed together with their mechanisms including processes between Ce^{3+} and Gd^{3+} ions. Finally, the characteristic properties of scintillating crystals based on perovskite structure are reviewed.

PACS numbers: 78.55.-m, 78.60.-b

1. Introduction

Recent applications of scintillators in medical imaging of human body (PET scanning, γ -cameras and X-ray tomographies) require improved or even quite new scintillating materials [1-7]. One of the most studied materials are either Ce^{3+} -doped crystals [1, 5, 6] or Ce^{3+} -concentrated ones as e.g. CeF_3 [8]. From various Ce^{3+} -doped crystals the most promising ones are orthoaluminates as $YAlO_3$ (YAP) [3, 9], $GdAlO_3$ (GAP) [10], $LuAlO_3$ (LuAP) [11, 12] and the mixed ones as e.g. $Y_xLu_{1-x}AlO_3$. The newest results of the studies of local structures of Ce^{3+} centres in YAP:Ce crystals were presented by us in [13] and the latest ones on the mixed $Lu_xGd_{1-x}AlO_3:Ce$ crystals in [14].

Ce^{3+} -doped $RE^{3+}AlO_3$ orthoaluminates are new types of crystal scintillators which are characterized by (i) high density (from ≈ 6 g/cm³ to 8.5 g/cm³), (ii) high light yield exceeding that of $Bi_4Ge_3O_{12}$ (BGO) which is roughly 9000 photons/MeV [3] and (iii) fast fluorescence and scintillation decays ($\tau \approx 10$ -30 ns) [3, 6, 11]. If the crystals have these properties together with mechanical and chemical stability then they can be used in scintillator applications as e.g. in PET

scanning where fast timing and high counting rate, good energy resolution and high stopping power are necessary.

In this paper we present the newest data and properties of the above given new kinds of scintillators having the perovskite structure. Intrinsic Ce^{3+} fluorescence and scintillation decay lifetimes of these crystals are in the time range 10–30 ns due to $\text{Ce}^{3+} 5d \rightarrow 4f$ allowed transitions. Energy transfer processes between Ce^{3+} main sites and multisites or from or to Ce^{3+} impurity ions are discussed together with their mechanisms. Finally, we summarise the basic fluorescence and scintillation properties of these crystals having the perovskite structure.

2. Experimental

Various experimental spectroscopic and scintillation techniques have been used for detailed characterization of $\text{RE}^{3+}\text{AlO}_3:\text{Ce}$ crystals. Computer controlled spectrophotometer Edinburgh Instruments Model 199S has been used for fluorescence spectra and decay studies in the spectral range 200–800 nm and in the time range ≈ 5 ns to 3 ms, respectively. Scintillation studies (emission spectra and decays) were carried out under excitation by 511 keV of ^{22}Na radiation.

Studied $\text{RE}^{3+}\text{AlO}_3:\text{Ce}$ ($\text{RE}^{3+} = \text{Y}^{3+}$, Gd^{3+} and Lu^{3+}) crystals or the mixed ones were grown by the company Preciosa Crytur Ltd in Turnov, Czech Republic (the crystals were grown by the Czochralski method). Ce concentrations in these crystals are not high, the maximum concentration reached is 0.6 at.% in YAP:Ce crystal. Generally, Ce concentrations are around 0.1–0.2 at.% Ce. The distribution coefficient of Ce^{3+} in these crystals is not high due to a difference between ionic radii of Ce^{3+} and the lattice ions Y^{3+} , Gd^{3+} and Lu^{3+} . The real Ce concentrations were evaluated by electron beam excited X-ray microanalysis which was carried out at the electron microscope JEOL.

Among many results on various scintillator crystals including $\text{RE}^{3+}\text{AlO}_3:\text{Ce}$ ones some of them have been found by the “Crystal Clear Collaboration” (CCC or RD18 project of CERN which is “Research & Development (R&D) for the study of new fast and radiation hard scintillators for calorimeter at Large Hadron Collider”). CCC collaboration co-ordinates the efforts of many laboratories and firms in finding and producing scintillators for various applications including new generation of electromagnetic calorimeter at CERN, medical imaging applications etc.

3. Spectroscopic and kinetic properties of Ce^{3+} in $\text{RE}^{3+}\text{AlO}_3$ crystals

Ce^{3+} energy levels in crystals consist of two ground state $4f$ levels (arising from one $4f$ electron) separated roughly by about 2000 cm^{-1} ($^2F_{5/2}$ and $^2F_{7/2}$) and up to five $5d$ split excited state energy levels (arising from $2D$ state of free Ce^{3+} ion)[1]. Separation of $4f$ and $5d$ energy levels in crystals depends strongly on local crystal fields and is ranging from ≈ 20000 to 35000 cm^{-1} for different crystals. $\text{Ce}^{3+} 5d \rightarrow 4f$ fluorescence transitions are the allowed ones (electric dipole–dipole) and their fluorescence lifetimes are in the time range 10–100 ns. Due to local changes of the crystals field (e.g. due to additional impurities in crystals, vacancies, local distortions in crystals etc.) various Ce^{3+} inequivalent centres arise

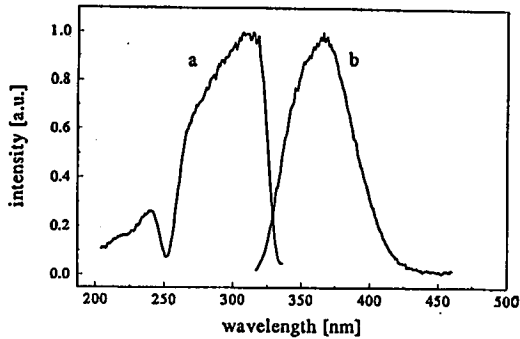


Fig. 1. Excitation (a) and emission (b) spectra of mixed $Y_xLu_{1-x}AlO_3:Ce$ crystal ($x = 0.94$, Ce concentration ≈ 0.08 at.%) at room temperature.

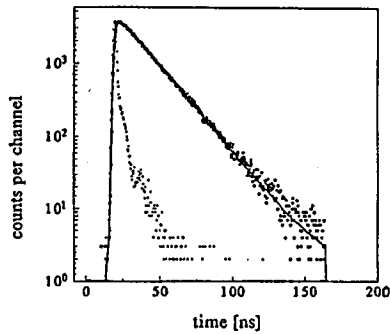


Fig. 2. Fluorescence decay curve of mixed $Y_xLu_{1-x}AlO_3:Ce$ crystal ($x = 0.94$, Ce concentration ≈ 0.08 at.%) at room temperature under $\lambda_{ex} = 300$ nm for $\lambda_{em} = 360$ nm. Decay curve is single exponential with lifetime $\tau \approx 17.7$ ns.

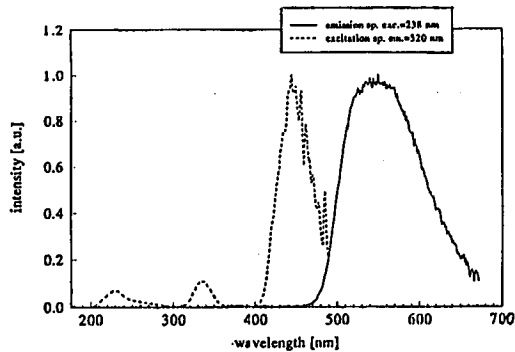


Fig. 3. Excitation (---) and emission (—) spectra of $Lu_3Al_5O_{12}:Ce$ at room temperature. This phase appears if contents of Y and Lu are the same (50 weight%) in raw materials from which the crystals were grown.

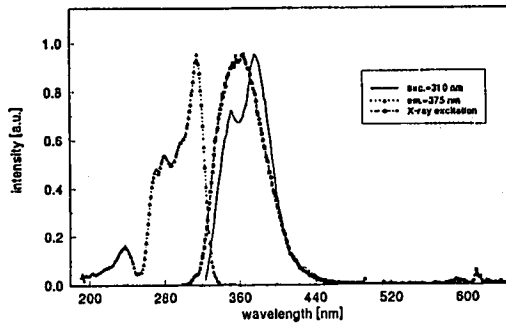


Fig. 4. Excitation and emission spectra of mixed $\text{Lu}_x\text{Gd}_{1-x}\text{AlO}_3:\text{Ce}$ crystal (for $x = 0.91$ and Ce concentration ≈ 0.16 at.%) at room temperature.

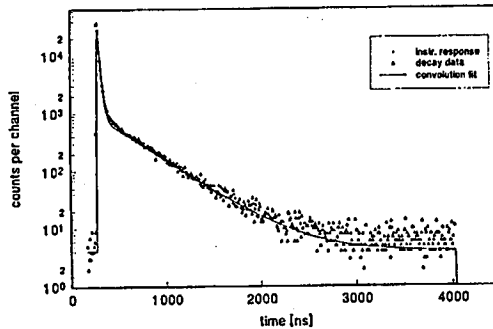


Fig. 5. Fluorescence decay curve of mixed $\text{Lu}_x\text{Gd}_{1-x}\text{AlO}_3:\text{Ce}$ crystal (for $x = 0.91$ and Ce concentration ≈ 0.16 at.%) at room temperature under $\lambda_{\text{ex}} = 320$ nm for $\lambda_{\text{em}} \approx 370$ nm. Double exponential convolution fit with lifetimes $\tau_1 \approx 20.5$ ns and $\tau_2 \approx 405$ ns was observed.

which results in additional fluorescence of these centres and processes of energy transfer in crystals.

In this paper we will present and summarise mainly the results of our studies of spectroscopic and kinetic properties of the mixed $\text{RE}^{3+}\text{AlO}_3:\text{Ce}$ ($\text{RE}^{3+} = \text{Y}^{3+}$, Gd^{3+} and Lu^{3+}) crystals. The experimental results are sketched in Figs. 1–8. Ce^{3+} emission and excitation spectra of the mixed $\text{Y}_x\text{Lu}_{1-x}\text{AlO}_3:\text{Ce}$ crystals (see Fig. 1) are roughly the same as those of pure $\text{YAP}:\text{Ce}$ crystals up to $x = 0.715$ ($\lambda_{\text{em}} \approx 370$ nm and $\lambda_{\text{ex}} \approx 310$ nm as the main emission and excitation maxima). If x exceeds 0.715 then yellow $\text{Lu}_3\text{Al}_5\text{O}_{12}:\text{Ce}$ garnet phase arises and its emission and excitation spectra are given in Fig. 3 ($\lambda_{\text{em}} \approx 550$ nm and various $5d$ excitation bands are observed in the spectral range 200–500 nm peaking at $\lambda_{\text{ex}} \approx 430$ nm at room temperature). Ce^{3+} fluorescence decay of $\text{Lu}_3\text{Al}_5\text{O}_{12}:\text{Ce}$ garnet $\tau \approx 60$ ns is a bit longer in comparison with the mixed $\text{Y}_x\text{Lu}_{1-x}\text{AlO}_3:\text{Ce}$ crystals where pure exponential decay is observed having lifetime $\tau \approx 17.7$ ns (see Fig. 2).

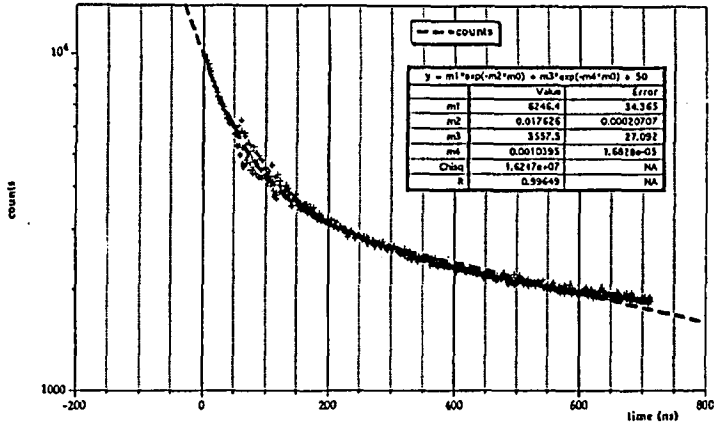


Fig. 6. Spectrally unresolved scintillation decay curve of mixed $\text{Lu}_x\text{Gd}_{1-x}\text{AlO}_3:\text{Ce}$ crystal (for $x = 0.91$ and Ce concentration ≈ 0.16 at.%) at room temperature (excitation by 511 keV γ -radiation of ^{22}Na source, $\lambda_{em} \approx$ whole Ce^{3+} emission band). Besides the fast Ce^{3+} component in the short part of decay the longer one can be evaluated by two exponentials having lifetimes $\tau_1 \approx 57 \mu\text{s}$ and $\tau_2 \approx 0.96 \text{ ms}$.

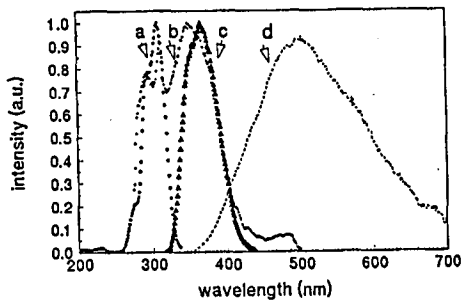


Fig. 7. Excitation (a) and emission (b, c) spectra of $\text{LuAlO}_3:\text{Ce}$ crystal (Ce concentration ≈ 0.04 at.%) at room temperature for $\lambda_{em} = 380 \text{ nm}$ (curve a), for X-ray excitation (curve b, Mo anticathode, 35 kV) and for $\lambda_{ex} = 290 \text{ nm}$ (curve c). The X-ray excited emission spectrum of BGO crystal (curve d) was taken under the same conditions as that of $\text{LuAlO}_3:\text{Ce}$ crystal (curve c) also at room temperature.

Excitation and emission spectra of the mixed $\text{Lu}_x\text{Gd}_{1-x}\text{AlO}_3:\text{Ce}$ crystal (for $x = 0.91$) are given in Fig. 4 for relatively high Ce content (≈ 0.16 at.%). Up to five Ce^{3+} excitation bands have been observed having maximum at $\lambda_{ex} \approx 310 \text{ nm}$ but Ce^{3+} emission spectra under UV and X-ray excitation are different. Under UV excitation a splitting of Ce^{3+} ground state of about $\approx 2000 \text{ cm}^{-1}$ is observed at room temperature. Fluorescence decay or scintillation decay curves of $\text{Lu}_x\text{Gd}_{1-x}\text{AlO}_3:\text{Ce}$ crystal are sketched and evaluated in Figs. 5 and 6, respectively. Under UV excitation (Fig. 5) two decay components are observed, the fast one is

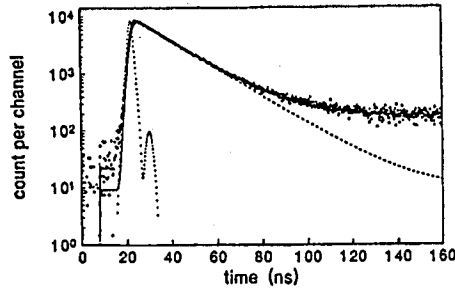


Fig. 8. Spectrally unresolved scintillation decay curve of $\text{LuAlO}_3:\text{Ce}$ crystal (Ce concentration ≈ 0.04 at.%) at room temperature (excitation by 511 keV γ -radiation of ^{22}Na source, $\lambda_{\text{em}} \approx$ whole Ce^{3+} emission band). The reconstructed instrumental response is given by smaller dots. The dashed line is the convolution of the instrumental response with a single exponential with decay time $\tau \approx 17.9$ ns. The solid line is the convolution of the instrumental response with a sum of two exponentials with $\tau_1 \approx 16.9$ ns and $\tau_2 \gg 1 \mu\text{s}$, the ratio of the preexponential factors (amplitudes) of the two components is $A_1/A_2 \approx 6.2$.

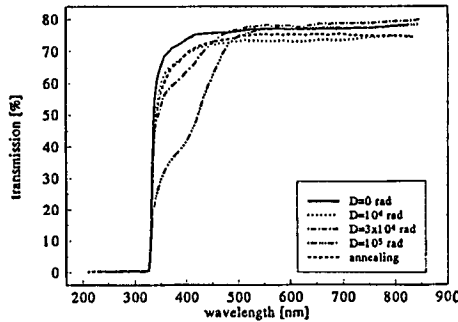


Fig. 9. Radiation damage testing of pure $\text{YAP}:\text{Ce}$ crystal up to 10^5 rad dose.

$\tau_f \approx 20.5$ ns, the slow one is $\tau_{sl} \approx 405$ ns. Under γ -ray excitation (by 511 keV radiation of ^{22}Na source) besides the fast component two slow decay components are observed with lifetimes $\tau_{sc}(1) \approx 57 \mu\text{s}$ and $\tau_{sc}(2) \approx 0.96$ ms.

Excitation and emission spectra of pure $\text{LuAlO}_3:\text{Ce}$ crystal (for Ce concentration ≈ 0.04 at.%) were described in [11] in detail and here are sketched in Fig. 7. Again, we can observe a difference between emission spectra excited under UV radiation and under X-rays (curves *c* and *b* in Fig. 7, respectively). The narrow emission bands in the UV peaking at $\lambda_1 \approx 288$ nm and $\lambda_2 \approx 308$ nm arise probably due to Gd^{3+} transitions ${}^6I_{7/2} \rightarrow {}^8S_{7/2}$ or ${}^6P_{7/2} \rightarrow {}^8S_{7/2}$, respectively. Also, the slowest decay lifetime from Fig. 7 is very close to Gd^{3+} lifetime ($\tau_{sl}(2) \approx 0.96 \mu\text{s}$ and $\tau(\text{Gd}^{3+}) \approx 2.3$ ms). Scintillation decay curve of $\text{LuAlO}_3:\text{Ce}$ crystal is sketched and evaluated in Fig. 8. Again, we can observe the fast decay component $\tau_f \approx 19.9$ ns and the slow one $\tau_{sl} \gg 1 \mu\text{s}$.

At present time scintillating crystals are tested upon their radiation hardness. Transmissions of pure YAP:Ce crystal under irradiation up to dose $D = 10^5$ rad are sketched in Fig. 9. These first results have shown that the radiation hardness of this crystal is not sufficient because additional absorption band appears at $\lambda_{ad} \approx 410$ nm both for YAP:Ce crystal and for the mixed $\text{Lu}_{0.91}\text{Gd}_{0.09}\text{AlO}_3:\text{Ce}$ crystal. The additional absorption bands arise probably due to colour or colour-related centres in these crystals [15].

4. Discussion and conclusions

Spectroscopic properties of Ce^{3+} ions in $\text{RE}^{3+}\text{AlO}_3:\text{Ce}$ ($\text{RE}^{3+} = \text{Y}^{3+}, \text{Gd}^{3+}$ and Lu^{3+}) crystals including the mixed ones are characterized by broad emission, excitation and absorption bands having their maxima in the near UV. The emission spectra of the main Ce^{3+} sites (Ce^{3+} ions replacing RE^{3+} lattice ions) are peaking generally at about $\lambda_m \approx 360\text{--}370$ nm but additional less intense emission bands are observed in the visible range, especially for YAP:Ce and GAP:Ce single crystals [3, 16]. Fluorescence lifetimes of these visible emission bands are very fast ($\tau \approx 15\text{--}20$ ns) if decays are excited in their own excitation bands. We interpret these additional emission bands as arising due to inequivalent Ce^{3+} centres in perovskite crystal structures. Another possibility for interpretation of less intense Ce^{3+} emission bands are their correlation with Ce^{3+} EPR spectra which were carried out by us [13].

EPR spectra represent an effective method of the detailed studies of structure, lattice location and charge states of point defects and impurities in crystals. Ce^{3+} EPR spectra can be correlated with the detailed fluorescence studies of YAP:Ce crystals where various inequivalent Ce^{3+} centres are observed [3]. In YAP:Ce crystals the Ce^{3+} EPR spectrum consists of single intense line without hyperfine structure (details see in [13]) and additional less intense lines around the main one (their intensities are 100–1000 times in magnitude weaker in comparison with the main one). The main most intense Ce^{3+} EPR line can be attributed to Ce^{3+} ions occupying Y^{3+} positions in YAP crystals and the “satellite” lines can be ascribed to Ce^{3+} -based centres or as defect-related Ce^{3+} -centres induced by another local distortion of the local crystal field. The defect-related Ce^{3+} centres (inequivalent ones) can be correlated with the observed Ce^{3+} inequivalent centres emitting less intense fluorescence bands in the visible range. This correlation between Ce^{3+} fluorescence and EPR spectra has shown that in perovskite structures Ce^{3+} impurity ions create the main Ce^{3+} centres (Ce^{3+} replacing RE^{3+} lattice ions) and the minor Ce^{3+} centres (defect-related centres). Ce^{3+} main and minor centres have been observed in YAP:Ce and GAP:Ce crystals (not in LuAP:Ce or in the $\text{Y}_x\text{--Lu}_{1-x}$ or $\text{Lu}_x\text{--Gd}_{1-x}$ mixed ones)[11, 14].

Ce^{3+} excitation and absorption spectra of the main and minor centres in YAP:Ce or GAP:Ce crystals are different but they overlap in some spectral ranges. Detailed excitation spectra and fluorescence decay studies have shown that there is radiative energy transfer between Ce^{3+} main and minor centres both in YAP:Ce and GAP:Ce crystals [3, 16].

Detailed fluorescence decay studies of Ce^{3+} ions in LuAP:Ce and $\text{Lu}_x\text{Gd}_{1-x}\text{AP:Ce}$ crystals have shown (see Figs. 5, 6 and 8) that besides the fast

Ce^{3+} decay $\tau_f \approx 15-20$ ns the slow decay components appear. This is an evidence that Gd^{3+} ions play important role in $LuAP:Ce$ and $Lu_xGd_{1-x}AP:Ce$ crystals even for trace Gd^{3+} concentrations as was observed for pure $LuAP:Ce$ crystal [11]. Slow Ce^{3+} decay components ($\tau_{sl} > 300 \mu s$) in these crystals are probably due to emission coming separately from Gd^{3+} ions (if we excite Gd^{3+} ions directly) or due to energy transfer processes and interaction between Ce^{3+} and Gd^{3+} ions. Gd^{3+} narrow emission lines were observed in the X-ray excited emission spectrum of one of $LuAP:Ce$ crystals (see curve *b* in Fig. 7). In mixed $Lu_{0.91}Gd_{0.09}AP:Ce$ crystal which contains ≈ 0.16 at.% Ce an efficient energy migration among Gd^{3+} ions is effective and an subsequent capture at another Ce^{3+} acceptor centres can take place. Especially, in $GAP:Ce$ crystal where Gd^{3+} is lattice ion the processes of Ce^{3+} delayed fluorescence are present [16] as $(Ce^{3+})_i \rightarrow (Gd^{3+})_{n \text{ steps}} \rightarrow (Ce^{3+})_j$ multistep processes.

One of the most important parameters of scintillator crystals are fluorescence and scintillation lifetimes. While in $YAP:Ce$ crystal the Ce^{3+} scintillation lifetime is roughly twice longer in comparison with the fluorescence lifetime in $LuAP:Ce$ crystal the Ce^{3+} scintillation and fluorescence lifetimes are the same and both are very fast ($\tau \approx 17$ ns). This similarity of scintillation and fluorescence lifetimes in $LuAP:Ce$ show that scintillation mechanism in this crystal is quite different than that in $YAP:Ce$. We suppose that in $LuAP:Ce$ the scintillation process is the following: recombination of e^- (electrons) and h (holes) $Ce^{3+} + h \rightarrow Ce^{4+}$ followed by $Ce^{4+} + e^- \rightarrow (Ce^{3+})^{ex}$. This mechanism shows that in $LuAP:Ce$ the Ce^{3+} scintillation excitation processes are much faster than Ce^{3+} fluorescence decay processes (below ≈ 17 ns which is the Ce^{3+} fluorescence lifetime).

Another important parameter of scintillators is their radiation hardness. The first studies of an influence of γ irradiation on $YAP:Ce$ crystals (see Fig. 9) have shown that the additional absorption band appears peaking at around 410 nm but no influence of γ irradiation has been observed in Ce^{3+} fluorescence properties up to 10^5 rad dose. The additional "transient" absorption at around 410 nm is probably due to colour centres which arise in crystals under γ irradiation [15]. A similar effect was also observed for $Lu_xGd_{1-x}AlO_3:Ce$ crystals.

Detailed spectroscopic and scintillation studies of $RE^{3+}AlO_3:Ce$ ($RE^{3+} = Y^{3+}, Gd^{3+}$ and Lu^{3+}) crystals including the mixed ones can be summarized as following:

1. Ce^{3+} impurity ions create either the main Ce^{3+} centres (Ce^{3+} replacing RE^{3+} lattice ions) or minor Ce^{3+} centres in these crystals, especially in $YAP:Ce$ and $GAP:Ce$ crystals.
2. Ce^{3+} inequivalent centres (minor ones) emitting in the visible are also excited due to radiative energy transfer from the main Ce^{3+} in the UV emitting centres.
3. The fast components of Ce^{3+} decays arise due to $5d \rightarrow 4f$ transitions of Ce^{3+} ions and the mean fluorescence and scintillation lifetimes are in the range 1.5–30 ns.

4. The slow components of Ce^{3+} decays (delayed fluorescence) are due to processes of $Ce^{3+} \rightarrow Gd^{3+}$ energy transfer followed by migration through Gd^{3+} lattice or sublattice and subsequent trapping at some of Ce^{3+} acceptor ions. Also under selected excitation Gd^{3+} fluorescence can be observed.

At the end of this paper we present Table in which we compare properties of the studied $RE^{3+}AlO_3:Ce$ ($RE^{3+} = Y^{3+}, Gd^{3+}$ and Lu^{3+}) crystals with other important scintillating materials. We can conclude that from the scintillator crystals having perovskite structure the most promising crystal should be $LuAP:Ce$. At present time no large and mechanically stable $LuAP:Ce$ crystals have been prepared but intense efforts are concentrated to solve this problem by various groups and firms.

TABLE
Properties of some cerium-activated scintillators of $RE^{3+}AlO_3:Ce$ ($RE^{3+} = Y^{3+}, Gd^{3+}$ and Lu^{3+}) crystals in comparison with the used ones or some new developed. (BGO = $Bi_4Ge_3O_{12}$, YAP:Ce = $YAlO_3:Ce$, LuAP:Ce = $LuAlO_3:Ce$, GAP:Ce = $GdAlO_3:Ce$, LSO = $Lu_2SiO_5:Ce$)

Scintillator	NaI(Tl)	BGO	YAP:Ce	LuAP:Ce	GAP:Ce	LSO	CeF ₃
ρ [g/cm ³]	3.67	7.13	5.36	8.34	7.5	7.4	6.16
Emission peak [nm]	410	480	370	370	360	420	280
Lifetimes [ns]	230	300	$\tau_n \approx 17$ $\tau_{sc} \approx 28$	17	1.5–20	30–60	5–30
Radiation length [cm]	2.59	1.12	2.8	1.1	–	1.1	1.7
Rel. light yield % of NaI(Tl)	100	20	40	25–50	–	20–25	10

References

- [1] G. Blasse, *Chem. Mater.* **6**, 1465 (1994).
- [2] W. Rossner, B.C. Grabmaier, *J. Lumin.* **48/49**, 29 (1991).
- [3] S. Baccaro, K. Blazek, F. De Notaristefani, P. Maly, J.A. Mares, R. Pani, R. Pellegrini, A. Soluri, *NIM Phys. Res. A* **361**, 209 (1995).
- [4] P. Lecoq, *J. Lumin.* **60/61**, 948 (1994).
- [5] RetD for the study of new, fast and radiation hard scintillators for calorimetry at LHC/RD18 CERN/LHCC 96-19, Status Report/RD18, February 1996.
- [6] M. Ishii, M. Kobayashi, *Prog. Cryst. Growth Char. Mat.* **23**, 245 (1992).
- [7] J.A. Mares, *J. Appl. Spectr.* **62**, 71 (1995).
- [8] M. Nikl, J.A. Mares, E. Mihokova, K. Blazek, J. Lorincik, *J. Lumin.* **60/61**, 971 (1994).
- [9] C. Pedrini, D. Bouttet, C. Dujardin, B. Moine, H. Bill, *Chem. Phys. Lett.* **220**, 433 (1994).

- [10] J.A. Mares, C. Pedrini, B. Moine, K. Blazek, J. Kvapil, *Chem. Phys. Lett.* **206**, 9 (1993).
- [11] J.A. Mares, M. Nikl, J. Chval, I. Dafinei, P. Lecoq, J. Kvapil, *Chem. Phys. Lett.* **241**, 311 (1995).
- [12] M. Moszynski, D. Wolski, T. Ludziejewski, A. Lempicki, C. Brecher, D. Wisniewski, A.J. Wojtowicz, in: *Proc. Int. Conf. on Inorganic Scintillators and Their Applications, SCINT95*, Delft (The Netherlands) 1995, Eds. P. Dorenbos, C.W.E. van Eijk, Delft Univ. Press, 1996, p. 348.
- [13] H.R. Asatryan, J. Rosa, S.A. Smirnova, J.A. Mares, P. Maly, J. Kvapil, in: *Proc. Int. Conf. on Inorganic Scintillators and Their Applications, SCINT95*, Delft (The Netherlands) 1995, Eds. P. Dorenbos, C.W.E. van Eijk, Delft Univ. Press, 1996, p. 329.
- [14] J.A. Mares, M. Nikl, J. Chval, J. Kvapil, J. Giba, K. Blazek, in: *Proc. Int. Conf. on Inorganic Scintillators and Their Applications, SCINT95*, Delft (The Netherlands) 1995, Eds. P. Dorenbos, C.W.E. van Eijk, Delft Univ. Press, 1996, p. 344.
- [15] V.G. Baryshevsky, M.V. Korzhik, B.I. Minkov, S.A. Smirnova, A.A. Fyodorov, P. Dorenbos, C.W.E. van Eijk, *J. Phys., Condens. Matter* **5**, 7893 (1993).
- [16] J.A. Mares, M. Nikl, C. Pedrini, D. Bouttet, C. Dujardin, B. Moine, J.W.M. Verweij, J. Kvapil, *Radiat. Eff. Defects Solids* **135**, 369 (1995).